Journal Pre-proof

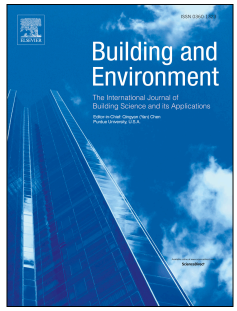

Modeling microclimatic effects of trees and green roofs/façades in ENVI-met: Sensitivity tests and proposed model library

Zhixin Liu, Ka Yuen Cheng, Tim Sinsel, Helge Simon, C.Y. Jim, Tobi Eniolu Marakinyo, Yueyang He, Shi Yin, Wanlu Ouyang, Yuan Shi, Edward Ng

PII: S0360-1323(23)00786-2

DOI: https://doi.org/10.1016/j.buildenv.2023.110759

Reference: BAE 110759

To appear in: *Building and Environment*

Received Date: 9 July 2023

Revised Date: 14 August 2023

Accepted Date: 20 August 2023

Please cite this article as: Liu Z, Cheng KY, Sinsel T, Simon H, Jim CY, Marakinyo TE, He Y, Yin S, Ouyang W, Shi Y, Ng E, Modeling microclimatic effects of trees and green roofs/façades in ENVI-met: Sensitivity tests and proposed model library, *Building and Environment* (2023), doi: https://doi.org/10.1016/j.buildenv.2023.110759.

Modeling microclimatic effects of trees and green roofs/façades in ENVI-met: Sensitivity tests and proposed model library

Zhixin Liu [a,b*], Ka Yuen Cheng [a], Tim Sinsel [c], Helge Simon [c], C.Y. Jim [d], Tobi Eniolu Marakinyo [e], Yueyang He [a,b], Shi Yin [f,g], Wanlu Ouyang [h,b], Yuan Shi [i], Edward Ng [a,b,j]

[a] *School of Architecture, The Chinese University of Hong Kong, New Territories, Hong Kong, China*

[b] *Institute of Future Cities, The Chinese University of Hong Kong, New Territories, Hong Kong, China*

[c] *Department of Geography, Johannes Gutenberg University Mainz, Mainz, Germany*

[d] *Department of Social Sciences and Policy Studies, The Education University of Hong Kong, New Territories, Hong Kong, China*

[e] *School of Geography, University College Dublin, Dublin, Ireland*

[f] *State Key Laboratory of Subtropical Building and Urban Science, South China University of Technology, Guangzhou, China*

[g] *School of Architecture, South China University of Technology, Guangzhou, China*

[h] *Department of Building and Real Estate, The Hong Kong Polytechnic University, Hong Kong, China*

[i] *Department of Geography & Planning, University of Liverpool, Liverpool, UK*

[j] *Institute of Environment, Energy and Sustainability, The Chinese University of Hong Kong, New Territories, Hong Kong, China*

* Corresponding author

Postal address: Room 505, Lee Shau Kee Architecture Building, The Chinese University of Hong Kong, Shatin, Hong Kong, China

Email address:

zhixinliu@cuhk.edu.hk (Zhixin Liu)

kayuencheng@cuhk.edu.hk (Ka Yuen Cheng)

t.sinsel@geo.uni-mainz.de (Tim Sinsel)

h.simon@geo.uni-mainz.de (Helge Simon)

cyjim@eduhk.hk (C.Y. Jim)

tobi.morakinyo@ucd.ie (Tobi Eniolu Marakinyo)

yueyanghe@cuhk.edu.hk (Yueyang He)

archyinshi@scut.edu.cn (Shi Yin)

wanlu.oy@link.cuhk.edu.hk (Wanlu Ouyang)

Yuan.Shi@liverpool.ac.uk (Yuan Shi)

edwardng@cuhk.edu.hk (Edward Ng)

Abstract:

Urban green infrastructure furnishes one of the most effective ways to mitigate and adapt to climate change and the consequent thermal environment deterioration. ENVI-met, a holistic computational fluid dynamics model with various plant modules, has become a principal simulation tool to evaluate the thermal effects of urban greenery. This study emphasized the significance of clear and accurate ENVI-met vegetation modeling, aiming to formulate strategies to boost modeling data quality, veracity and rigor of ENVI-met-based simulation studies. This study applied a two-step framework. First, a series of sensitivity tests were conducted under hot and humid meteorological conditions to identify the microclimate-sensitive parameters and their relative cooling effects at the pedestrian level. The results identified leaf area density as the most significant parameter in ENVI-met tree modeling. Some compromises on roof properties' input accuracy could be tolerated since they would not considerably hamper the overall simulation quality at the pedestrian level. For green roof/façade modeling, leaf area index and leaf angle distribution were significant and should be accurately input to ensure simulation quality. Second, for the microclimate-sensitive parameters in modeling, this study used commonly-planted species in subtropical South China cities to demonstrate a systematic workflow of developing an ENVI-met vegetation model library. The library could include basic plant physical traits, plant albums, reference values of the microclimate-sensitive parameters, and recommended alternative modeling data sources. The vegetation model library could provide a helpful and actionable package from which researchers can quickly obtain accurate input values without highly specialized knowledge or instruments.

Keywords: ENVI-met; Vegetation modeling; Microclimate; Urban tree; Green roof and façade; Model library

1. Introduction

In recent decades, many cities have suffered from urban warming, which can be attributed to the combined impacts of global climate change and the urban heat island (UHI) effect [1]. It leads to higher urban temperatures and more frequent extreme heat events, exacerbating heatwaves and human-health risks [2]. To mitigate and adapt to urban climate change, urban green infrastructure has been identified as one of the most significant *Nature-based Solutions* due to its considerable cost-effective cooling potential [3]. Through evapotranspiration and shade provision, plants can intercept 70–90% of incoming solar radiation, reduce 2−4 ℃ air temperature in parks, and reduce 11−22.4 ℃ peak building surface temperatures, depending on their physical traits and planting designs [4].

Meanwhile, with the significant advancements in computation resources in recent decades, numerical simulation has gradually become one of the principal research approaches to evaluate the thermal and human-biometeorological effects of urban greenery [5]. EBM-based (Energy Balance Models) models such as RayMan, SOLWEIG, green-CTTC, and CFD-based (Computational Fluid Dynamic) models such as OpenFOAM, FLUENT, PHOENICS, ENVI-met are commonly used tools to simulate greenery effects [6]. Compared to EBM-based models, CFD-based models offer a twofold advantage: explicit coupling simulation capability and high-resolution [7]; they have been widely applied to more urban greening-related studies [6]. Concerning plant representations in CFD-based models, PHOENICS and FLUENT employ the Ideal canopy model with a limited representation of a tree by its crown height, trunk height, and basic canopy geometry such as spherical, oval, or conical shape. OpenFOAM, the FOLIAGE module of PHOENICS, employs the Statistical method by associating LAI with plant morphology [5]. With various plant modules and detailed in-canopy radiation calculations, ENVI-met can provide a more accurate and detailed plant characterization. It has been used in over half of the greenery-led urban cooling simulation studies [6].

ENVI-met is a holistic three-dimensional CFD model developed by Michael Bruse in 1998. With solid physical fundamentals based on fluid mechanics, thermodynamics, and atmospheric physics laws, ENVI-met can simulate surface-plant-air interactions in high resolution [8-11]. Currently, ENVI-met has four plant modules: *simple plants* for grass and hedges; *green roof/façade module* for roof/façade greenings on building envelopes; *3D-plants*, and *Lindenmayer-Systems* for trees. *Simple plants* represent vegetation as one-dimensional columns featuring adjustable values for albedo, transmittance and plant height. Each column consists of ten layers of LAD (leaf area density) and RAD (root area density). *Green roof/façade module* combines buildings, greenings, and substrates, making it possible to consider heat and vapor exchanges among greenery, substrate, and building surface layers. In green roof/façade modeling, plant species can be edited by dragging and dropping a *simple plant* into the green roof/façade. The main greening properties are plant thickness, LAI (leaf area index), and leaf angle distribution. Properties such as albedo and transmittance of the vegetation are copied from the selected *simple plants*, while other properties only fitting to individual plants, such as plant height, LAD and RAD, are omitted for the design of a roof/façade greening. The substrate is optional and requires data on its properties, including emissivity, albedo, water coefficient for plants, and air gap thickness between the substrate and wall (Fig. 1).

In tree modeling, 3D trees allow a plant-as-object simulation and can be digitized in a three-dimensional plant editing tool named *Albero* [11], in which tree geometry, leaf properties, and root zone geometry are needed (Fig. 1). The latest version (V5) of ENVI-met, released in November 2021, includes the *Lindenmayer-Systems tree*. It can describe the more realistic position and arrangement of leaf clusters and an hierarchical tree branching system [12]. Besides the advancements in vegetation modeling, a new ACRT (advanced canopy radiation transfer) module in V5 allows diffuse radiation extinction simulations and secondary sources of diffuse radiation due to the scattering of direct shortwave radiation within vegetation canopies [12]. Recent developments in modeling and calculation have brought estimates of greening-related microclimates closer to reality.

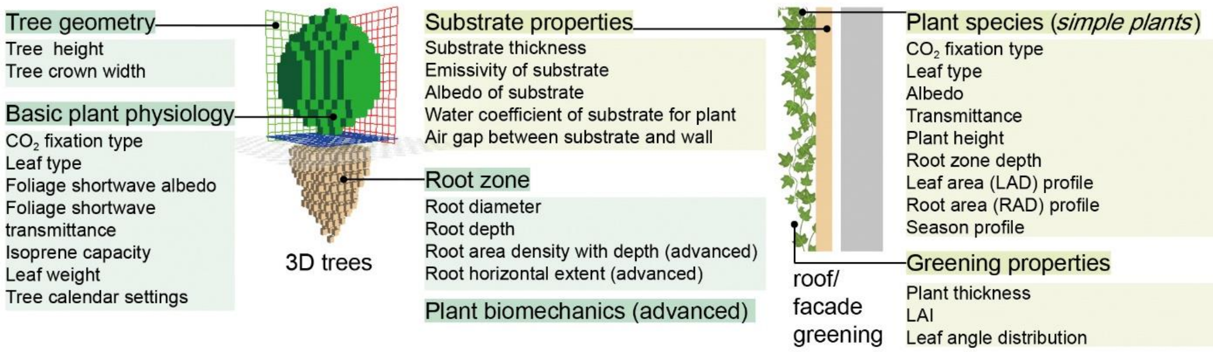

Fig. 1. Modeling parameters of ENVI-met 3D trees and roof/façade greening.

Due to the diversity of vegetation models and the complexity of plant-atmosphere-building interactions in ENVI-met, the importance of model accuracy cannot be overstated. The more detailed and accurate plant models are, the better ENVI-met can denote reality. Previous validation studies have summarized that modeling assumption as one of the primary reasons causing deviations between simulated and observed values, including but not limited to assumed input data and greenery generalization in study domains [5, 13, 14].

Four approaches are commonly adopted to acquire physical plant properties in ENVI-met modeling. These include citing literature, actual measurements, parameterizing according to physical plant characteristics, and selecting existing vegetation models from the ENVI-met built-in library [5]. Liu et al. [5] recommended using real data in modeling; however, they are not easy to obtain due to the limited data sources. ENVI-met has provided default values in its modeling platform and listed various vegetation models in the built-in library for users' selection. Still, two issues in ENVI-met vegetation modeling have remained inadequately understood:

(1) Which greening physical parameters are the microclimate simulation results more sensitive to and therefore demand the most accurate input values? Which parameters could accept a high tolerance for errors in estimating their numerical values if insufficient input data sources exist? To what extent will the approximations affect microclimate?

(2) Most plant species in the ENVI-met built-in library are from temperate climate regions. However, the physical traits of plants vary tremendously in different climate regions and subregions. A tailor-made ENVI-met vegetation model library for a specific climate zone is needed.

To solve these pending issues, this study aims to formulate strategies for ENVI-met vegetation modeling to boost modeling data quality, simulation veracity, and rigor of ENVI-met studies. Sensitivity tests were performed to investigate modeling parameter sensitivity to microclimate at the pedestrian level. Also, this study applied common plant species in subtropical South China as an example to show a systematic workflow of developing an ENVI-met vegetation model library.

2. Literature review of ENVI-met vegetation modeling

A condensed literature review was attempted to understand the state of ENVI-met greenery modeling studies. This literature review aimed to ascertain the frequently employed modeling parameters and those that tended to be disregarded in ENVI-met vegetation modeling. The literature-searching approach used in a previous work [5] was adopted in this study. All included articles applied ENVI-met V4 and above as the main research tool to evaluate the improvement of the outdoor thermal environment with urban greenery. As plant characteristics vary tremendously among climate regions, only studies in the temperate climate zone with a hot and humid summer (classified as *Cfa* in the Köppen-Geiger climate classification [15]) were included. In total, 47 peer-reviewed English journal articles were reviewed. Only half of the reviewed studies (25, 53.2%) selected specific plant species, while the remaining parameterized vegetation according to generic physical traits.

In digitizing specific tree species, most studies reported the use of tree height (18, 85.7%), followed by crown diameter (15, 71.4%) and foliage density (12, 57.1% studies reported LAI and 10, 47.6% studies reported LAD). Only a few studies reported bole height (5, 23.8%), foliage shortwave albedo (3, 14.3%), foliage shortwave transmittance (2, 9.5%), and leaf type (4, 19.0%). None of the studies mentioned root-related properties. Model input data sources can be categorized twofold: single data source and mixed data source (model settings that were partially modified from a single source based on researchers' demands would be classified as a mixed data source). About half of the specific tree species-related studies (11, 52.4%) acquired tree properties from a single data source, including actual measurements (9, 42.9%), citing literature (1, 4.8%), and selecting existing tree models from *Albero* (1, 4.8%). One-third of the studies (7) chose mixed data sources. Among them, six studies (28.6%) set vegetation models based on their study foci, such as mid-size trees. Three studies (14.3%) didn't report any data source.

Regarding the green roof/façade, only studies that used ENVI-met V4.4 and above were examined. Until then, users had to place *simple plants* in front of buildings to replicate façade greening. However, this approximation approach is no longer used because the dedicated new green roof/façade module can consider the heat and vapor exchanges within and between the greenery and substrate layers [5]. This study calculated the input data for green roofs and vertical greening modeling together due to the same module (four studies). In *simple plants* modeling, the LAD profile was frequently reported (3, 75.0%). Plant height, albedo, and root properties such as root depth and RAD profile were reported by two studies (50.0%). Only one study (25.0%) mentioned transmittance. In terms of the greening properties in the green roof/façade module, LAI, plant thickness, and leaf angle distribution were respectively reported by 75.0% (3), 50.0% (2), and 75.0% (3) studies. Unlike tree modeling's data sources, most green roof/façade studies acquired data from the literature (2, 50.0%) rather than actual measurements (0, 0%). One study only reported partial data sources (from the literature). In another study, the authors defined modeling input values based on their research aims.

Only one reviewed study modeled specific shrub/grass species [16], reporting plant height and LAD selected from ENVI-met built-in library.

In reviewing the previous ENVI-met vegetation modeling procedures, three observations could be addressed. First, the modeling process should be described more comprehensively. The essential information should be reported in detail, including modeling settings, values, and data sources that may significantly influence the simulation results. Second, actual measurements should be the primary data source in modeling specific tree species. It is an accurate approach to digitizing a representative tree, but it has limits, such as being time-consuming and demanding professional instruments. Among tree modeling parameters, physical traits such as tree height and crown diameter can be easily obtained by tape measures or laser rangefinders, so most studies reported them. However, the more sophisticated tree parameters were reported only by a few reviewed studies, probably due to no access to expensive and professional instruments. This may explain the use of parameterized tree models rather than modeling specific tree species in about half of the reviewed studies. Third, in green roof/façade modeling, there were fewer studies focusing on specific plant species than tree studies. This is because the new green roof/façade module was released only four years ago. However, the lack of professional instruments for measuring some plant physical traits is similar to tree studies. The reviewed studies usually introduced plant modeling but omitted substrate descriptions. Substrates may influence the magnitude of the green roof/façade's thermal effect, considered the main analytical aspect in relevant studies [17].

The literature review reveals that systematic scientific strategies for proper ENVI-met vegetation modeling are urgently needed. Currently, the varied modeling data sources in reviewed studies were based on researchers' measurements or literature surveys. The appropriation and accuracy of modeling input values demand attention, particularly for microclimate-sensitive parameters. A tailor-made ENVI-met vegetation model library can facilitate and save time for ENVI-met users.

3. Methods

3.1. Study framework

This study has two broad stages: sensitivity tests and developing an ENVI-met vegetation model library. The sensitivity tests aim to investigate the magnitude of each vegetation modeling parameter's microclimate influence. The ENVI-met vegetation model library aims to provide a helpful and actionable package for users. An overview of the methodological framework is depicted in Fig.2. The study area was set to Hong Kong (22 °15 ' N, 114°10' E), a high-density metropolis in a humid subtropical climate with a *Cfa* Köppen-Geiger climate classification [18]. All ENVI-met simulations were performed using the V5.0 Science version.

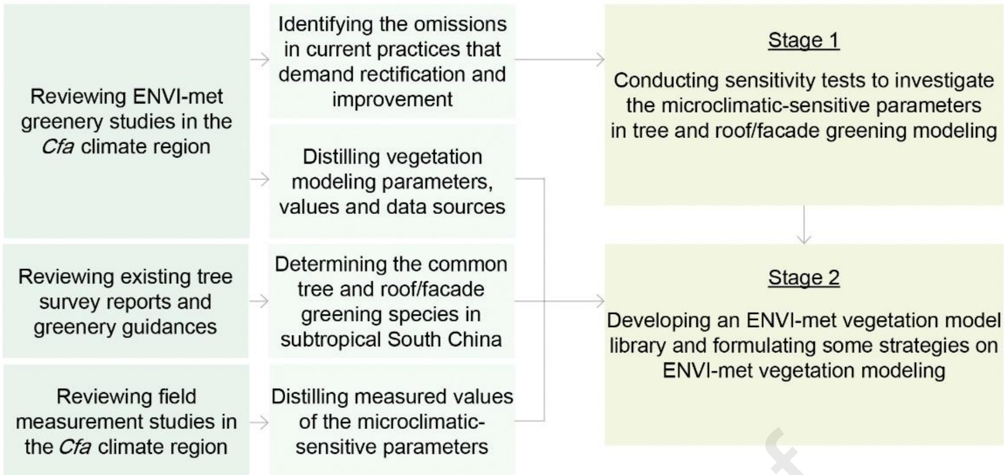

Fig. 2 The methodological framework of this study.

3.2. Sensitivity tests

3.2.1. Sensitivity test method determination

A sensitivity test, also known as a sensitivity analysis, is a method used to assess the sensitivity or responsiveness of a system or model to changes in its input parameters or assumptions. There are four commonly-used experiment methods: randomization designs, one-factor-at-a-time (1FAT) designs, full factorial designs, and orthogonal fractional factorial designs [19]. Referring to relevant research [20], this study selected the 1FAT method because it is widely applied in both academic and industrial design of experiments courses and can help isolate and understand the influence of each factor independently [21]. This study applied three levels of each modeling parameter, i.e., high, medium, and low, to build a series of test cases.

3.2.2. Test cases

3.2.2.1. Tree models

Four parameters, including LAD, foliage shortwave albedo, root depth, and root diameter, were tested in the tree sensitivity tests. All sample trees' height and crown diameter were respectively set as 10 m and 8 m, referring to the general size of *Acacia confusa* [22], which is the most frequently planted tree species in Hong Kong public housing estates [23] and tree management information systems [24]. The omission of tree dimensions in the sensitivity analysis in this study was based on the assumption that landscape practitioners can easily obtain accurate measurements of tree height and crown width using simple and inexpensive tools such as tape measures or laser rangefinders, while the main focus of this study was to investigate the impact of modeling parameters that are less easily obtained on microclimate. In this study, three levels of LAD, foliage shortwave albedo, root depth, and root diameter, were set referring to the ENVI-met built-in tree library. The maximum, minimum, and average values of the 29 tree species in the library were applied as the high, low, and medium levels in sensitivity tests. In terms of foliage shortwave transmittance, due to the constant value (0.30) in the ENVI-met built-in library, this study referred to the transmittance of crops to set the low (0.10) and high levels (0.52) [25]. The tree samples were categorized twofold: one *standard tree* was modeled through medium levels of all input parameters, and ten *test trees* were modeled by varying one parameter into a higher or lower class. The values of each test case are listed in Table 1. The size of the simulation domain was 40 m×40 m×30 m with 1 m resolution in the X, Y, and Z axis (Fig. 3(a) (b)). All test trees were planted in the center of an open loamy soil area to maximize their microclimatic effects. In vertical grid generation, the lowest gridbox was split into five subcells.

Tree height, bole height, and crown diameter were not included in sensitivity tests for the following reasons. First, their accurate values can be obtained through measure tapes or rangefinders, which are affordable for researchers and landscape practitioners. Second, the significant influences of these tree physical traits on tree shade provisions and surrounding microclimate have been found by many studies [26-28].

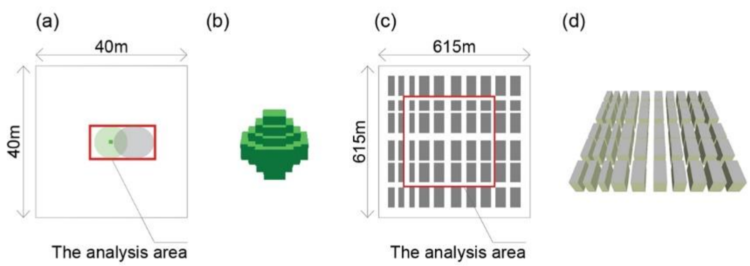

Fig. 3 The ENVI-met models of the test cases (a) 2D model of the tree cases (the grey circle represents the tree shading at 15:00 h), (b) 3D model of the tree cases, (c) 2D model of the façade greening cases, and (d) 3D model of the façade greening cases.

Table 1. The modeling values of each tree test case.

Test cases	**LAD of each grid cell (m^2/m^3)**	**Foliage shortwave albedo**	**Foliage shortwave transmittance**	**Root diameter (m)**	**Root depth (m)**
The standard tree (all medium levels)	1.15	0.44	0.31	14	10.4
The test tree (high-level LAD)	2.00	0.44	0.31	14	10.4
The test tree (low-level LAD)	0.3	0.44	0.31	14	10.4
The test tree (high-level albedo)	1.15	0.70	0.31	14	10.4
The test tree (low-level albedo)	1.15	0.18	0.31	14	10.4
The test tree (high-level transmittance)	1.15	0.44	0.52	14	10.4
The test tree (low-level transmittance)	1.15	0.44	0.10	14	10.4
The test tree (high-level root diameter)	1.15	0.44	0.31	25	10.4
The test tree (low-level root diameter)	1.15	0.44	0.31	3	10.4
The test tree (high-level root depth)	1.15	0.44	0.31	14	20.0
The test tree (low-level root depth)	1.15	0.44	0.31	14	0.8

3.2.2.2. Green roof/façade models

Regarding roof/façade greening, the sensitivity tests had two aspects: *simple plants* in roof/façade greening and roof/façade greening properties. The former tested five parameters, including *simple plants*' albedo, transmittance, root zone depth, LAD and RAD; the latter tested six parameters, including LAD, leaf angle distribution, emissivity of substrate, albedo of substrate, water coefficient of substrate for plant, and air gap thickness between substrate and wall. Similar to trees, the physical traits of all roof/façade greening samples were set consistently. The plant height of all *simple plants* samples was consistently set as 0.4m. The plant thickness, substrate thickness, and substrate materials of all roof/façade greening samples were respectively set as 0.3m, 0.15m, and sandy loam.

Three levels of input parameters were applied in the roof/façade greening modeling. Due to the similarity of the ENVI-met built-in green roof/façade models, input values of leaf albedo, leaf transmittance, LAI, emissivity and albedo of the substrate from Ref. [29] were applied to set the high, low, and medium levels. Regarding leaf angle distribution, 0 means the leaf is parallel to the façade, and 1 is perpendicular following the ENVI-met Database Manager. Considering the extreme values cannot be set in ENVI-met, this study applied 0.9, 0.5, and 0.1 to the high, medium, and low levels of leaf angle distribution. The water coefficient of substrate for plants is a dimensionless factor that determines the water availability of plants, ranging from 0 (no water available) to 1 (full water accessible for plants). This study set it to 0.9, 0.5, and 0.1. Regarding the air gap width between the substrate and wall, the maximum and minimum values in the ENVI-met built-in library are 0.10 m and 0.01 m. Therefore, a medium level of 0.06 m was set in sensitivity tests. The values of each *simple plants* and roof/façade greening test case are listed in Tables 2 and 3.

Table 2. The modeling values of each *simple plants* test case.

***Simple plant* models**	**Albedo**	**Transmittance**	**Root zone depth (m)**	**LAD profile (10 layers) (m^2/m^3)**	**RAD profile (10 layers) (m^2/m^3)**
The standard simple plant (all medium level)	0.28	0.24	0.35	0.32	0.15
The test simple plant (high-level albedo)	0.36	0.24	0.35	0.32	0.15
The test simple plant (low-level albedo)	0.20	0.24	0.35	0.32	0.15
The test simple plant (high-level transmittance)	0.28	0.30	0.35	0.32	0.15
The test simple plant (low-level transmittance)	0.28	0.18	0.35	0.32	0.15
The test simple plant (high-level root zone depth)	0.28	0.24	0.50	0.32	0.15
The test simple plant (low-level root zone depth)	0.28	0.24	0.20	0.32	0.15
The test simple plant (high-level LAD)	0.28	0.24	0.35	0.48	0.15
The test simple plant (low-level LAD)	0.28	0.24	0.35	0.15	0.15
The test simple plant (high-level RAD)	0.28	0.24	0.35	0.32	0.20
The test simple plant (low-level RAD)	0.28	0.24	0.35	0.32	0.10

Table 3. The modeling values of each roof/façade greening test case.

Green roof/façade models	**LAI (m^2/m^2)**	**Leaf angle distribution**	**Emissivity of substrate**	**Albedo of substrate**	**Water coefficient of substrate for plant**	**Air gap between substrate and wall (m)**
The standard green roof/façade (all medium level)	3.15	0.5	0.93	0.28	0.5	0.06
The test green roof/façade (high-level LAI)	4.8	0.5	0.93	0.28	0.5	0.06

The test green roof/façade (low-level LAI)	1.5	0.5	0.93	0.28	0.5	0.06
The test green roof/façade (high-level leaf angle distribution)	3.15	0.9	0.93	0.28	0.5	0.06
The test green roof/façade (low-level leaf angle distribution)	3.15	0.1	0.93	0.28	0.5	0.06
The test green roof/façade (high-level emissivity of substrate)	3.15	0.5	0.95	0.28	0.5	0.06
The test green roof/façade (low-level emissivity of substrate)	3.15	0.5	0.90	0.28	0.5	0.06
The test green roof/façade (high-level albedo of substrate)	3.15	0.5	0.93	0.30	0.5	0.06
The test green roof/façade (low-level albedo of substrate)	3.15	0.5	0.93	0.26	0.5	0.06
The test green roof/façade (high-level water coefficient of substrate for plant)	3.15	0.5	0.93	0.28	0.9	0.06
The test green roof/façade (low-level water coefficient of substrate for plant)	3.15	0.5	0.93	0.28	0.1	0.06
The test green roof/façade (high-level air gap between substrate and wall)	3.15	0.5	0.93	0.28	0.5	0.10
The test green roof/façade (low-level air gap between substrate and wall)	3.15	0.5	0.93	0.28	0.5	0.01

In ENVI-met, the model domain was 615 m×615 m×130 m with a 3 m resolution in the X, Y, and Z axis (Fig. 3(c) (d)). A generic layout plan based on the urban morphology of Mong Kok, Hong Kong [18] was applied. The widths of streets between buildings were 10, 15, 20, and 30 m. The building heights were homogeneous at 60 m (the mean building height of the area [18]), and the aspect ratio varied from 2 to 6, representing typical urban morphology characteristics in high-rise and high-density Hong Kong. Besides, considering the medium or low-density urban areas, another model with a 20 m building height and 0.5 to 1.5 aspect ratio was built. In ENVI-met models, telescoping grids were applied in vertical space, with a telescoping factor of 15% and started after 10 m. Vertical greenings were set in all building envelopes to maximize their microclimatic effects. Since this study focused on the thermal and human-biometeorological impact of urban greenery at the pedestrian level, green roofs were not tested since Sinsel et al.[30] reported that the cooling effect of green roofs has limited elevation distribution and may cease at building heights of around 100 m.

3.2.3. ENVI-met initialization

Simulations ran for 17 hours for all test cases, starting at 01:00 h and ending at 18:00 h. To maximize the microclimatic effects of urban greenery, the hourly meteorological data of the hottest summer day in 2019 (9^{th} August) from the Hong Kong Observatory (HKO) were applied in the full-forcing module (listed in Appendix A). The IVS (indexed view sphere) module was applied with 45° resolution. Tmrt (mean radiant temperature) used the common six-directional approach. The ACRT module was turned on to calculate the attenuated and scattered direct shortwave radiation within plants.

3.2.4. Data analysis

Eight microclimatic parameters (i.e., air temperature, specific humidity, wind speed, Tmrt, direct shortwave radiation, diffuse shortwave radiation, reflected shortwave radiation, and wall surface temperature) and one basic human thermal comfort indicator (PET, physiological equivalent temperature) at the pedestrian level (1.5 m height) were extracted for further analysis. PET is a function of four main meteorological variables of Ta, RH, WS, and Tmrt, considering human elements such as gender, height, age, weight, clothing heat resistance, and metabolic heat [31, 32]. It is the most widely used indicator in urban climatology [33-36] and ENVI-met greenery-related studies [5]. The simulation results of 15:00 h were analyzed because it is the time when the maximum differences between the thermal comfort of open and vegetated areas generally occur [5], and the differences among test cases would be considerable. In the tree model tests, the analysis area was set as a rectangle of 12 m×8 m, involving the areas under the tree canopy and tree shading at 15:00 h (Fig. 3(a)). In the green roof/façade model tests, the analysis focused on the blocks' central area, avoiding unstable simulation results in outer block areas (Fig. 3(c)). Paired samples T-test was conducted in SPSS 24 [20] (117 paired samples were used in tree-related cases. 7985 and 1906 paired samples were respectively for the microclimate conditions and wall surface temperature at the pedestrian level in roof/façade greening cases). A 95% confidence interval percentage was applied.

3.2.5. ENVI-met validation

The authors' research team has previously conducted a series of urban greenery studies in hot and humid high-rise, high-density cities, where the suitability of the ENVI-met simulation model for urban microclimate was validated and demonstrated [13, 37-42]. A validation paper conducted by the authors' team concluded that ENVI-met effectively simulated air temperature and mean radiant temperature with satisfactory accuracy during summer daytime. The simulations also successfully replicated the thermal and radiative characteristics of various green infrastructures, such as ground trees, green facades, and green roofs [14]. Additionally, another validation study conducted by the authors' research team focused on evaluating ENVI-met's performance in simulating physiological parameters (leaf surface temperature and vapor flux) and thermal effects (solar radiation, air temperature, and humidity) of four commonly found tree species in southern China, reported that the ENVI-met tree model is suitable for subtropical hot-humid climates [13]. Based on the solid research foundation, it is accurate to apply ENVI-met as the primary simulation tool in this study.

3.3. Developing an ENVI-met vegetation model library

After determining the microclimatic-sensitive parameters from the sensitivity tests mentioned above, an ENVI-met vegetation model library was developed. It has two aspects: a tree library and a roof/façade greening library. Previous field measurement studies and ENVI-met greenery studies furnished the primary data sources.

3.3.1. Determining plant species in the library

Considering that common plant species may vary among climate regions, this study applied those in subtropical South China as an example to develop an ENVI-met vegetation model library. Roadside trees, public housing estate trees, and urban park trees in three typical cities in southern China, i.e., Hong Kong, Macau, and Guangzhou, were comprehensively surveyed during the last twenty years [23, 43-50], providing the primary data sources in this study. Frequency distributions of tree species were distilled from the published tree survey reports, from which the top 20 common tree species were analyzed.

Regarding roof/façade greening, due to the lack of detailed surveys like trees, this study referred to the *Pictorial Guide to Plant Resources for Skyrise Greenery in Hong Kong* [51]. The plant database was compiled by the *Greening and Landscape Office* in the *Development Bureau of the Hong Kong Government.* It could facilitate proper plant selections and encourage the installation of green roofs and vertical greening. This study distilled four main categories of roof/façade greenings, i.e., climber, succulent, grass, and fern, from the database. In total, 24 commonly-used plant species in roof/façade greenery were included in the library development.

3.3.2. Selecting data sources

The library's primary data source is the literature, including previous field measurement studies and ENVI-met greenery studies. The microclimate-sensitive parameters were used as keywords in literature searching, but only studies in the *Cfa* climate zone were selected because plant geometry varies among climate regions. Regarding ENVI-met greenery studies, the 47 studies reviewed in Section 2 were also applied here. In the library, species Latin or common names followed those reported in the original literature. Basic information, vegetation modeling parameters, corresponding values, data sources, and images were extracted in detail.

4. Results and discussion of sensitivity tests

4.1. Trees

The average differences between the two tree modeling levels (between the medium level and the high/low level, respectively) are displayed in Fig. 4 (detailed values listed in Appendix B). The light grey dash lines represent differences of 0.01 (for radiation-related variables, they represent differences of 1 W/m^2) because most microclimatic studies round to two decimal places. In the data analysis in this study, differences between the two levels of test cases lower than 0.01(1 for radiation) would be considered "no difference at all".

When LAD varied from medium to other levels, all microclimatic variables except air temperature showed notable changes. Therefore, due to its high microclimatic sensitivity, LAD must be accurate in ENVI-met tree modeling. In the ENVI-met ACRT module, attenuation of direct and diffuse shortwave radiation through vegetation grids follows the work of Pedruzo-Bagazgoitia et al. [12, 52], using three processes: 1) primary extinction of direct shortwave radiation; 2) extinction of direct shortwave radiation due to scattering and creation of secondary diffuse shortwave radiation; and 3) extinction of diffuse shortwave radiation. LAIc, i.e., the sum of LAI between the grid cells, is applied to all in-canopy radiation transfer calculations, revealing that LAI/LAD is an essential modeling parameter. The agglomerations of leaves, given by LAD, also have crucial effects on wind speed. According to Bruse et al. [8], in the ENVI-met atmospheric model, the loss of wind speed due to vegetation's drag forces is estimated by the mean wind speed at the height, plant's LAD at the height and the mechanical drag coefficient. LAD is the only plant parameter that affects wind speed due to the constant value of the mechanical drag coefficient (0.2). In terms of air temperature, however, the p-value of 0.74 was much greater than 0.05, revealing that the resulting air temperature difference is statistically insignificant when changing LAD from a medium to a higher level. This phenomenon was also reported by Liu et al. [13] in an ENVI-met validation study: the air temperature reduction from trees tends to be underestimated. But this is understandable since Brown et al. [53] stated that "air temperature and atmospheric humidity cannot normally be significantly modified by landscape elements" because "any localized changes you can make in air temperature will be quickly dissipated by air movement".

Foliage shortwave albedo only showed notable changes in reflected shortwave radiation, Tmrt, and PET. When foliage shortwave albedo varied from 0.44 (the medium level) to 0.7 (the high level), the average reflected shortwave radiation, Tmrt, and PET at the pedestrian level increased by 13.31 W/m^2, 0.44 ºC, and 0.19 ºC, respectively. There is a positive correlation between foliage shortwave albedo and reflected shortwave radiation. This result is due to the higher albedo, bringing more reflection of shortwave radiation to the atmosphere. In ENVI-met, Tmrt is by default estimated by the common six-directional approach since Version 5 [54], and, in the daytime, PET is affected mainly by Tmrt. This result is consistent with previous findings that shortwave radiation significantly affects human absorbed radiation flux and outdoor thermal comfort [55]. The foliage shortwave transmittance influences reflected shortwave radiation, Tmrt, and PET, but the trend was opposite to the foliage shortwave albedo. When the foliage shortwave transmittance changed from a medium level to a high level (from 0.31 to 0.52), the average reflected shortwave radiation, Tmrt, and PET at the pedestrian level decreased by 3.90 W/m^2, 0.41 ºC, and 0.19 ºC, respectively. For these two modeling parameters, the p-values of the direct shortwave radiation changes were greater than 0.05, revealing that in varying foliage albedo or transmittance, the resulting direct shortwave radiation differences were statistically insignificant. Also, there was no difference in diffuse shortwave radiation, revealing that foliage shortwave albedo and transmittance did not affect diffuse radiation estimation in ENVI-met simulations. These results were reasonable because, in ENVI-met, the major contributions to tree shading and radiation transfer are caused by the agglomeration of leaves, which is given by LAD [12].

Tree root depth and diameter did not significantly affect the microclimate at the pedestrian level. In varying the modeling levels, no statistically significant differences existed between the simulation results of Tmrt, PET, and all shortwave radiation-related variables (p-values were greater than 0.05). When changing root diameter, the average air temperature differences were statistically significant, but the difference value was quite low (about 0.0005 ºC), which can be considered no difference. But it should be noted that all tree samples in sensitivity tests were planted on loamy soil, providing well water availability for trees. The results may change if a pavement profile with drier materials is chosen.

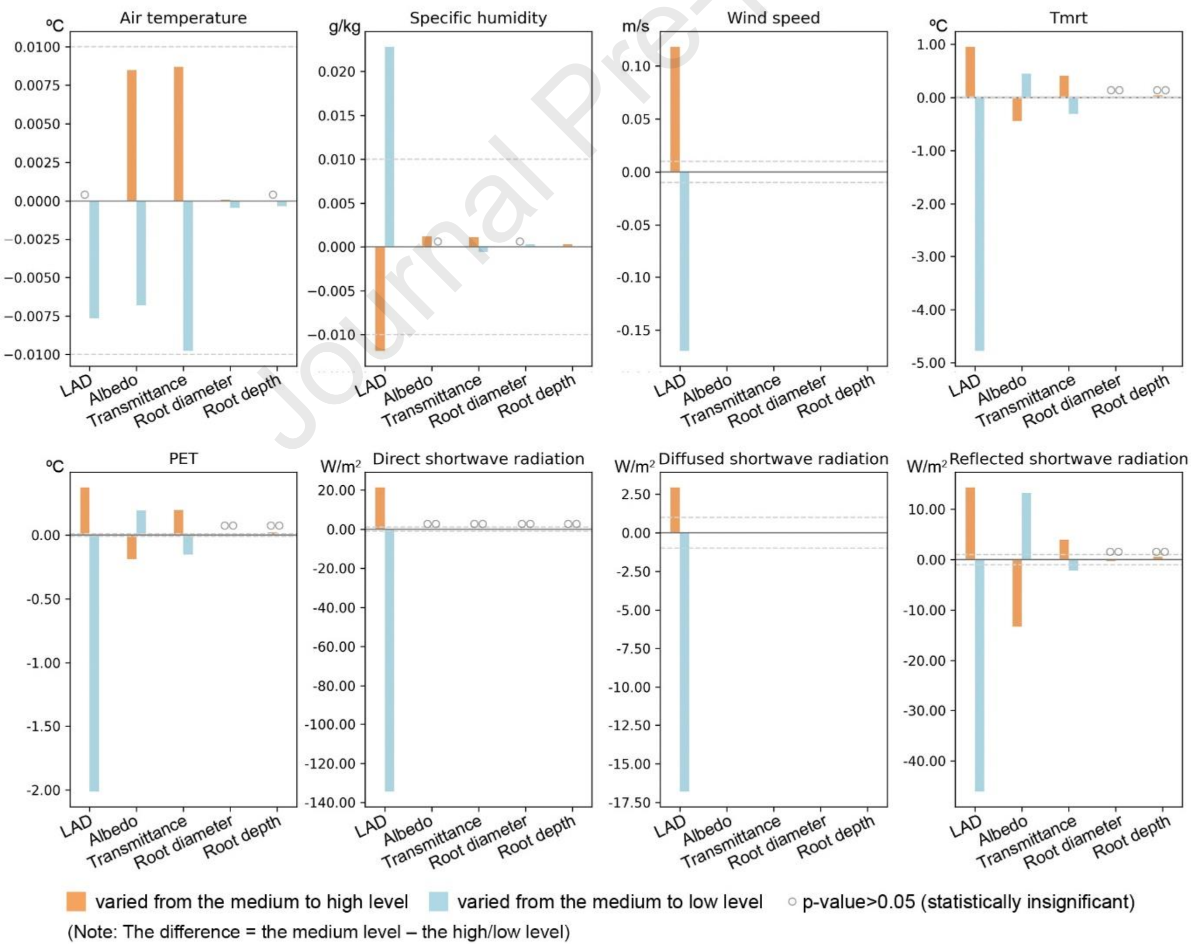

Fig 4. Mean microclimatic differences between two tree modeling levels.

4.2. Façade greening

The average differences between the two *simple plant* modeling levels are displayed in Fig. 5 (detailed values listed in Appendix C). Direct and diffuse shortwave radiation at the pedestrian level was not included in the diagram since there were no changes in all test cases. Due to the similar results, only façade greening in 60 m height buildings is discussed here in detail. The results of 20 m height buildings can be found in Appendix D.

Regarding the *simple plants* in a green roof/façade module, only plant albedo and transmittance (as well as C3/C4 CO_2 fixation type, not shown in this study) were involved in calculations. When changing transmittance to a lower level, the pedestrian level's air and wall surface temperature increased by 0.04 ºC. It is because the lower the transmittance, the higher the absorption (the albedo was set consistently), resulting in more absorbed heat of plants and a higher surrounding temperature through convection. Plant albedo and transmittance were not sensitive to specific humidity and wind speed, as shown by the very small variation of two parameters (ranging from 0.0006 to 0.007 g/kg in specific humidity, and from 0.0006 to 0.002 m/s in wind speed). This is because albedo and transmittance are radiation-related parameters and would not directly affect humidity and wind speed in ENVI-met. Due to the radiation budget changes within and behind the canopy, some tiny changes in specific humidity and wind speed could eventually be observed. Regarding root zone depth, LAD, and RAD, there was no difference in varying their modeling levels because these three parameters are not involved in simulation when *simple plants* have been placed in a green roof/façade module.

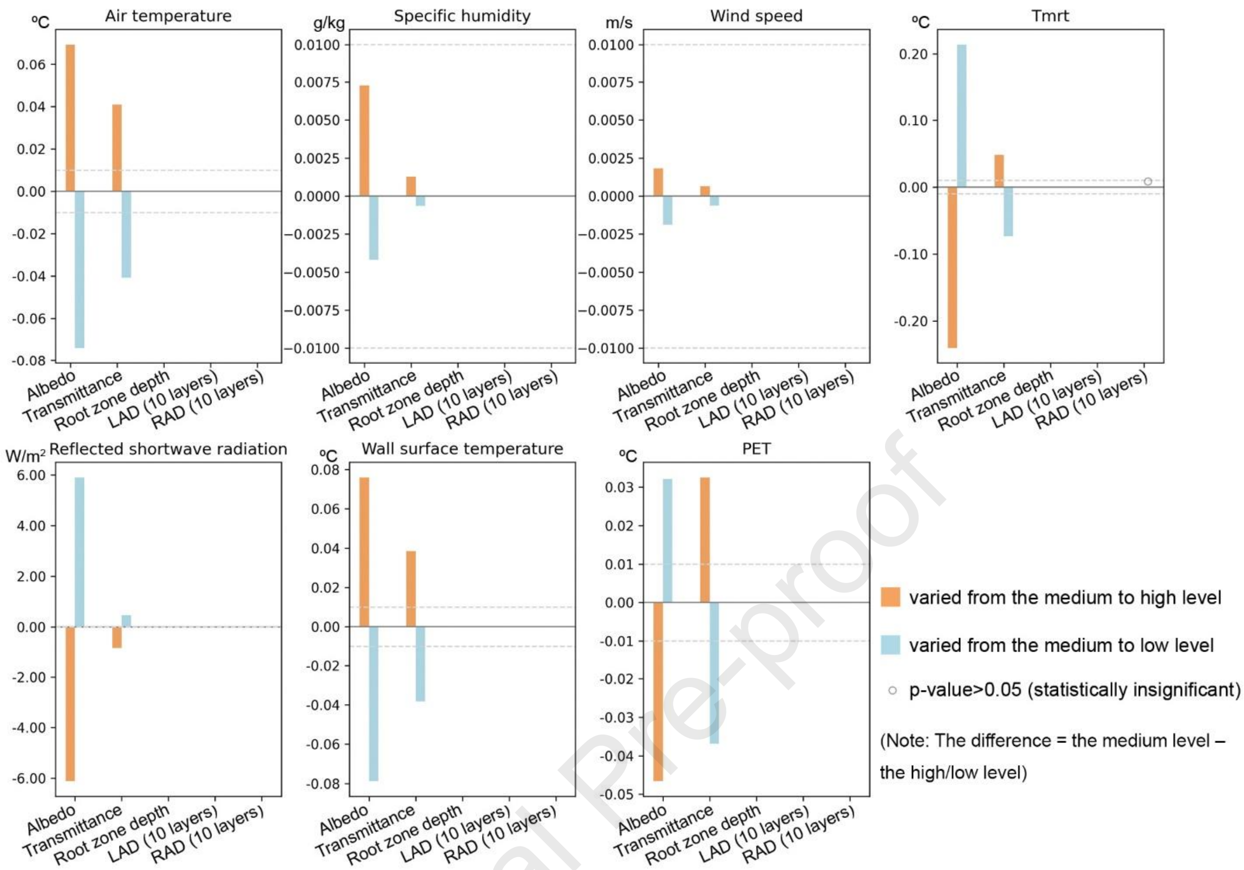

Fig 5. Mean microclimatic differences between two *simple plant* modeling levels in green façades.

Regarding modeling parameters in the green roof/façade module, the mean microclimatic differences between the two modeling levels are displayed in Fig. 6 (detailed values listed in Appendix E). Wind speed was not sensitive to all modeling parameters because it is mainly affected by urban morphology, such as building layouts and tree planting configuration. The plant thickness was only 0.3 m in this study, so, understandably, it has limited influence on street canyon air ventilation. In varying the greening properties (i.e., LAI and leaf angle distribution), all the microclimatic variables (except wind speed) showed significant differences. Particularly, PET was greatly influenced by these two modeling parameters (changes ranging from 0.37 to 0.84 ºC and 0.31 to 1.74 ºC for LAI and leaf angle distribution, respectively). The analysis would be conducted from the perspective of radiation transfer since most microclimatic variables here are relevant to radiation (e.g., reflected shortwave radiation, Tmrt, PET), particularly in the shortwave radiation domain.

In the ENVI-met green/façade module, a given fraction of the incoming shortwave radiation will not enter the façade greening system. Still, it will be scattered and reflected in the environment. The shortwave radiation released into the atmosphere contains three categories: 1) reflected direct shortwave radiation; 2) reflected diffuse shortwave radiation; and 3) transmitted shortwave radiation from the vegetation layer (radiation reflects from the wall or substrate layer and transmits through the vegetation layer to release back into the atmosphere). The reflected shortwave radiation in the direct and diffuse components are estimated by incoming direct/diffuse shortwave radiation, the vegetation layer's direct/diffuse absorption coefficient and albedo. The direct/diffuse absorption coefficient is related to leaf angle distribution, LAD (estimated from LAI and plant thickness), and the optical thickness of the vegetation layer for the direct/diffuse component (related to the vegetation thickness). Estimating the transmitted shortwave radiation from the vegetation layer involves leaf transmittance, leaf angle distribution, vegetation thickness, and LAD. The abovementioned analysis elaborates on the significance of simple plant-radiation properties (plant albedo and transmittance) and plant structural properties (LAI and leaf angle distribution) in ENVI-met radiation estimation. For leaf angle distribution, this phenomenon is in line with previous studies: leaf angle distribution plays a crucial role in intra- and inter-canopy microclimate, controlling energy and mass balance in the soil-vegetation-atmosphere-transfer system [56].

Regarding substrate properties, the substrate emissivity greatly impacted wall surface temperature (ranging from 0.59 ºC to 0.88 ºC upon changing to a higher or lower level). This result is understandable since the higher the substrate emissivity, the more energy would emit to the surroundings, resulting in a higher wall surface temperature. Substrate albedo is involved in the substrate-reflected shortwave radiation estimation. But its effect was relatively slight (only about 1.27 W/m^2 differences when changing to a higher or lower level) because most shortwave radiation transfer occurs between the vegetation layer and the atmosphere. Changing the substrate's water coefficient level brought relatively considerable shifts in air temperature and specific humidity (ranging from 0.03 to 0.14 ºC and 0.05 to 0.24 g/kg, respectively). Since the substrate layer can be seen as soil materials, the turbulent fluxes of heat and vapor in the substrate layer can be estimated according to Ref. [8]. Neglecting horizontal transfers, the soil can be treated as a horizontal column with heat and soil volumetric moisture content distributions and can interact with the atmosphere. The air gap width had no notable effect on microclimate at the pedestrian level since almost all interactions occur among air, vegetation layer, and a substrate layer. Also, the substrate blocks all the radiation (both shortwave and longwave domains) and cannot reach the wall surface.

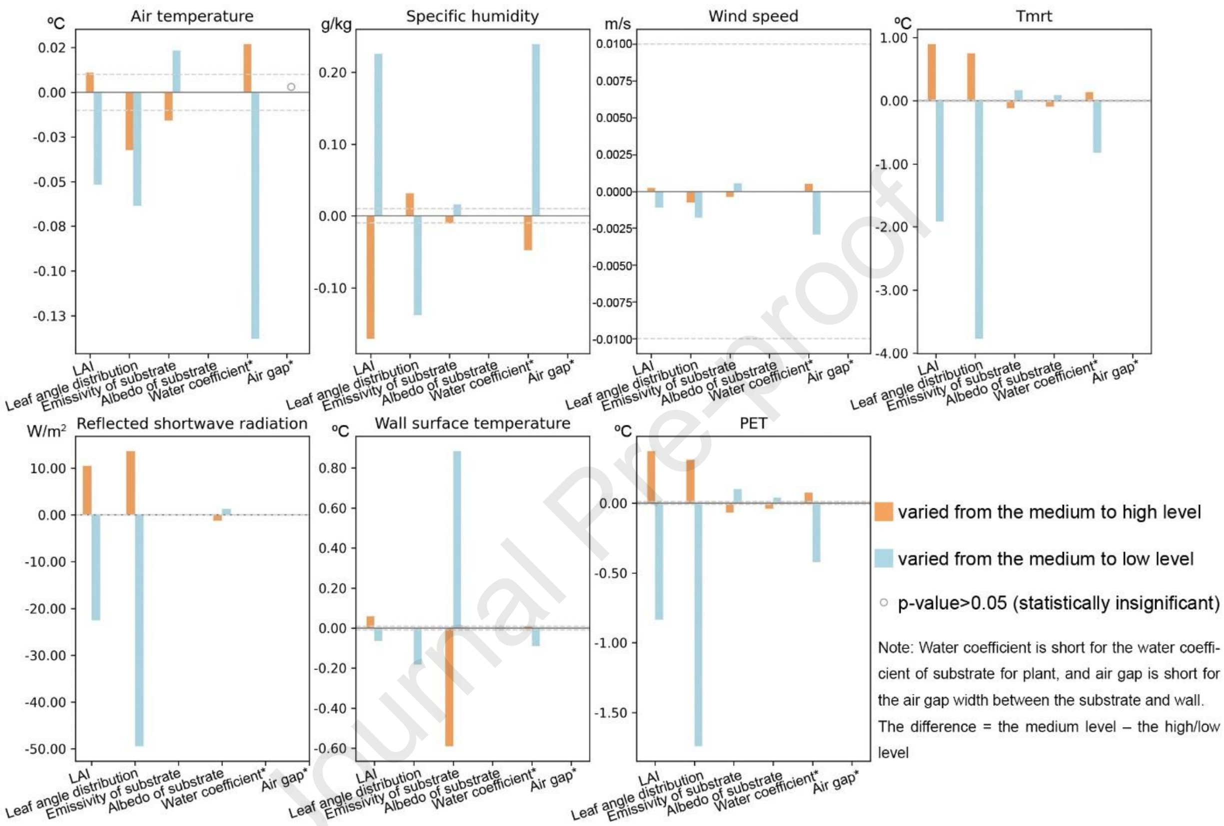

Fig 6. Mean microclimatic differences between two green façade modeling levels.

5. ENVI-met vegetation model library

The structure of the proposed ENVI-met vegetation model library is displayed in Fig. 7.

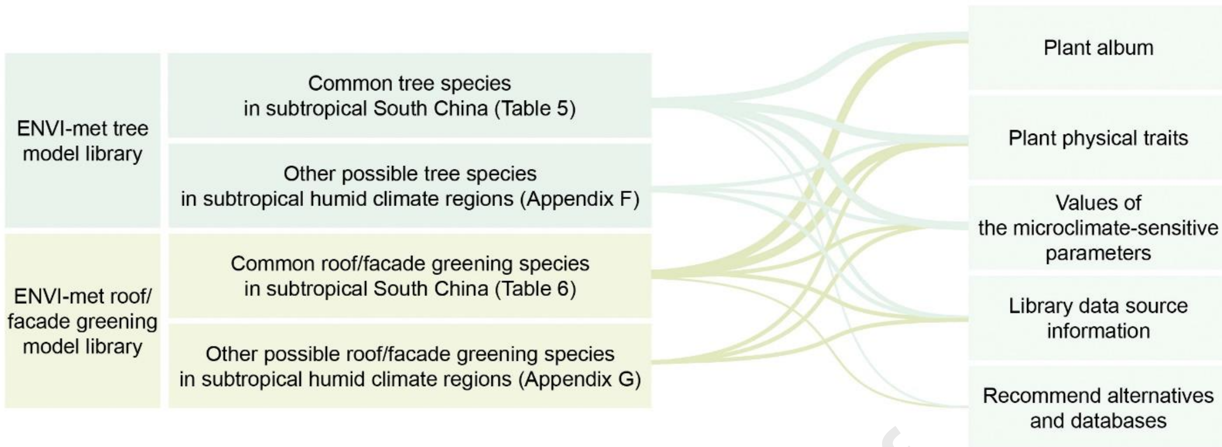

Fig. 7. The structure of the proposed ENVI-met vegetation model library.

5.1. Tree model library

Based on the tree survey reports in the last 20 years [23, 43-50], the main characteristics of the top 20 common tree species in subtropical South China were distilled (Table 4). The dominant tree species were *Acacia confusa*, *Ficus microcarpa,* and *Bauhinia x blakeana*, with frequencies considerably greater than other tree species (64,550, 37,867, and 34,488 trees, respectively). 75% of these common tree species were evergreen trees, so there is no need to edit the seasonal scale factor in *Tree Calendar* for these trees in ENVI-met *Albero*. The average and large tree sizes were extracted from Ref. [22, 57], with the values representing tree dimensions in current and future scenarios, respectively. However, their appropriateness in future studies should be carefully assessed since the data sources were the tree surveys in Hong Kong's public housing estates [22, 57].

Table 4. Main characteristics of the common tree species planted in subtropical South China cities.

Rank	**Tree species**	**Family**	**Foliage retention**	**Frequency**	**Average size**		**Large size**	
					Height	**Crown width**	**Height**	**Crown width**
1	*Acacia confusa*	Mimosaceae	Evergreen	64,550	9.8	8.2	15.9	17.7
2	*Ficus microcarpa*	Moraceae	Evergreen	37,867	8.3	9.6	16.1	22.7
3	*Bauhinia x blakeana*	Caesalpiniaceae	Evergreen	34,488	7.4	6.5	13.6	12.5
4	*Melaleuca cajuputi subsp. cumingiana*	Myrtaceae	Evergreen	28,530	10.5	5.1	-	-

5	*Macaranga tanarius*	Euphorbiaceae	Evergreen	26,950	6.1	7.1	10.9	14.4
6	*Casuarina equisetifolia*	Casuarinaceae	Evergreen	25,099	15.0	8.4	-	-
7	*Livistona chinensis*	Arecaceae	Evergreen	24,572	-	-	25.6	19.4
8	*Aleurites moluccana*	Euphorbiaceae	Evergreen	23,345	10.2	7.4	17.3	14.3
9	*Ficus virens*	Moraceae	Deciduous	17,947	10.2	10.9	18.7	22.6
10	*Schefflera heptaphylla*	Araliaceae	Evergreen	17,323	-	-	11.4	10.5
11	*Lagerstroemia speciosa*	Lythraceae	Deciduous	17,145	5.4	5.3	10.9	9.3
12	*Celtis sinensis*	Ulmaceae	Deciduous	16,780	8.4	8.0	16.3	16.1
13	*Bauhinia variegata*	Caesalpiniaceae	Deciduous	16,585	7.5	6.4	13.9	11.9
14	*Sterculia lanceolata*	Sterculiaceae	Evergreen	15,171	-	-	11.2	12.3
15	*Cinnamomum camphora*	Lauraceae	Evergreen	14,276	9.1	7.8	15.6	17.5
16	*Delonix regia*	Caesalpiniaceae	Deciduous	13,268	8.9	11.0	16.7	22.0
17	*Lophostemon confertus*	Myrtaceae	Evergreen	10,967	-	-	14.4	12.3
18	*Melaleuca leucadendra*	Myrtaceae	Evergreen	10,203	-	-	-	-
19	*Eucalyptus spp.*	Myrtaceae	Evergreen	9,849	-	-	23.1	15.4
20	*Mallotus paniculatus*	Euphorbiaceae	Evergreen	9,779	-	-	14.2	12.7

The ENVI-met tree model library for the common tree species is displayed in Table 5. Due to the lack of relevant literature, five tree species (*Schefflera heptaphylla*, *Celtis sinensis*, *Bauhinia variegata*, *Eucalyptus spp.*, and *Mallotus paniculatus*) were not included in the current library. Except for the top 20 common tree species, modeling information of other possible tree species mentioned in the reviewed literature was also recorded for users' reference (Appendix F).

The first step in applying the library is choosing the most appropriate information. Since there could be several pieces of modeling information for a given tree species, users must select the most appropriate one based on their needs. This library provided detailed tree physical traits, tree albums, and data source information. Also, if the crown diameter and bole height information are not included in that piece, tree photographs in the original literature or the tree album included in this study (Fig. 8) can be used as ballpark references. Users can roughly estimate them from the proportions of the tree shape. The source of tree images is the *Plant Photo Bank of China* (http://ppbc.iplant.cn/). Here, to provide readers with a relatively accurate visual reference of tree form, photographs of individual mature trees were selected, minimizing the influence of surrounding buildings and other plants on the tree's shape. However, this study encourages readers to conduct extensive research and gain knowledge about the morphology of the specific tree species before modeling.

Fig. 8 Tree album for the common tree species planted in subtropical South China cities.

Based on the abovementioned sensitivity tests, LAD, foliage shortwave albedo, and transmittance are microclimate-sensitive. In the library, tree height and LAI values were ascertained. It is because although LAD is the most essential modeling parameter, it is difficult to measure precisely. Thus, it is usually estimated by an empirical formula using LAI and tree heights [58]. Very few studies reported foliage shortwave albedo and transmittance. It is understandable because leaf albedo was generally measured from spectrophotometers [13] or two albedometers [59, 60], which are expensive and relatively inaccessible to some extent. Approximations from ENVI-met built-in library or literature findings from other climate regions (included in Appendix F) could provide alternatives, but their appropriateness needs to be carefully assessed before use. The influence of approximation can refer to the sensitivity test results mentioned above. Some researchers used a smartphone application called *Albedo: a Reflectance App* to measure material albedo in situ [61]. However, whether this application suits foliage albedo measurement is still unclear. In terms of foliage shortwave transmittance, it is sometimes confused with “tree canopy transmissivity” in some studies. Defined by the radiative transmissivity of a single leaf, an approximation of 0.3 is offered by ENVI-met as a default setting based on previous measurement studies [62, 63].

It should be noticed that in ENVI-met tree modeling, “deciduous leaves” should be chosen in the “Basic Plant Physiology” panel in *Albero,* whether it is an evergreen or deciduous tree in Table 4. In ENVI-met, the leaf type (grass leaves, deciduous leaves, and conifer leaves) is used for a specific aerodynamic resistance calculation, in which different leaf types have different plant-specific constants and leaf diameters (leaf diameters 0.15 m for deciduous trees and 0.02 m for conifers and grass) [11, 64]. Plant aerodynamic resistance is essential since it would be used for all sensible heat flux, latent heat flux, and evapotranspiration calculations.

Some useful data sources are recommended, offering researchers a direction to obtain modeling data. LAI and tree maximum height, tree form, and other basic tree information can be found on the Singapore Flora&Fauna Web (https://www.nparks.gov.sg/florafaunaweb). The LAI values in that database are for Green Plot Ratio calculation, which can provide a practical data source for ENVI-met modeling for tropical climates. For the common tree species in residential areas in Guangzhou, China (*Michelia alba*, *Mangifera indica*, *Ficus microcarpa*, and *Bauhinia x blakeana*), detailed modeling information such as tree size, leaf albedo, LAI, LAD profile, even root depth and width can be found in Ref. [13].

Table 5. An ENVI-met tree model library for the top 20 common tree species planted in subtropical South China cities.

No.	Tree species	Tree physical trait: Height (m)	Crown diameter (m)	Bole height (m)	DBH (cm)	Microclimate-sensitive modeling parameter: LAI (m^2/m^2)	LAD at each layer (m^2/m^3)	Foliage shortwave albedo	Tree photo in original literature	Data source: Data source category*	ENVI-met version (if any)	City	Country	Ref.	Note
1		12.5	-	-	-	2.5	-	-	-	EN-fm	4	Hong Kong	China	[65]	-
2		12.3	-	-	-	2.5	-	-	-	FM	-	Hong Kong	China	[65]	Raw data from measurement
3	*Acacia confusa*	10.0	16.0	1.8	60	2.40	-	-	✓ Hemispheric	FM	-	Hong Kong	China	[66]	-
4		8.92	6.00	-	24	3.0	-	-	✓ Front	LIT	-	Hong Kong	China	[67]	LAI in the intermediate canopy
5		10	-	-	-	3	-	-	-	EN-fm	4	Hong Kong	China	[65]	-
6		9.6	-	-	-	3.14	-	-	-	FM	-	Hong Kong	China	[65]	Raw data from measurement
8		7.8	18.0	1.8	78	2.81	-	-	✓ Hemispheric	FM	-	Hong Kong	China	[66]	-
9		8.1	11.0	1.3	-	-	Listed	0.31	✓ Front	FM	-	Guangzhou	China	[55]	-
10		8.1	11.0	1.3	-	3.88	Listed	0.31	✓ Front	EN-fm	4.2	Guangzhou	China	[13]	-
11		7 – 15	-	-	-	1.26 – 4.44	-	-	-	EN-fm	≥4	Guangzhou	China	[68]	-
12	*Ficus microcarpa*	7 – 15	-	-	-	1.26 – 4.44	-	-	-	EN-fm	4.4.4	Guangzhou	China	[69]	-
13		10	9	-	-	2	-	-	-	EN-set	4.4.4	Guangzhou	China	[69]	-
14		5.50	6	2	18.98	3.43	Listed	0.31	✓ Front	EN-mix	4.2	Guangzhou	China	[26]	From the regression model of measurement
15		8 – 13	7 – 15	-	-	3.45 (summer) 3.21 (autumn) 3.02 (winter)	-	-	-	EN-fm	4.3.2	Shenzhen	China	[70]	-
16		10	9	-	-	2	-	-	-	EN-mix	4.3.2	Shenzhen	China	[70]	-
17		7.5	-	-	-	3	-	-	-	EN-fm	4	Hong Kong	China	[65]	-
18		7.3	-	-	-	2.84	-	-	-	FM	-	Hong Kong	China	[65]	Raw data from measurement
19		7.2	6.0	2.0	24	3.55	-	-	✓ Hemispheric	FM	-	Hong Kong	China	[66]	-
20	*Bauhinia × blakeana*	4.9	5.8	-	-	3.55	-	-	✓ Front	LIT	-	Hong Kong	China	[71]	-
21		14.4	9.4	1.6	-	-	Listed	0.31	✓ Front	FM	-	Guangzhou	China	[55]	-
22		8.8	9.1	1.8	-	4.27	Listed	0.31	✓ Front	EN-fm	4.2	Guangzhou	China	[13]	-

23		14.4	9.4	1.6	-	4.17	Listed	0.31	✓ Front	EN-fm	4.2	Guangzhou	China	[13]	-
24		6.82	6	2	14.87	3.02	Listed	0.31	✓ Front	EN-mix	4.2	Guangzhou	China	[26]	From the regression model of measurement
25		7	6	2	-	3.55	-	-	✓ Hemispheric	EN-fm	4	Hong Kong	China	[37, 72]	-
26		10	-	-	-	2	-	-	-	EN-fm	4	Hong Kong	China	[65]	-
27	*Melaleuca cajuputi* subsp. *cumingiana*	11.7	-	-	-	2.14	-	-	-	FM	-	Hong Kong	China	[65]	Raw data from measurement
28		8.65	3.79	-	24	3.0	-	-	✓ Front	LIT	-	Hong Kong	China	[67]	LAI in the intermediate canopy
29		4.2	8.0	1.2	25	3.02	-	-	✓ Hemispheric	FM	-	Hong Kong	China	[66]	-
30	*Macaranga tanarius*	5.2	8.0	-	-	3.02	-	-	✓ Front	LIT	-	Hong Kong	China	[71]	Named as *Macaranga tanarius* var. *tomentosa* in the original literature
31		4	8	1	-	3.02	-	-	✓ Hemispheric	EN-fm	4	Hong Kong	China	[37, 72]	-
32		11.2	6.0	6.2	20	2.11	-	-	✓ Hemispheric	FM	-	Hong Kong	China	[66]	-
33	*Livistona chinensis*	9.0	5.6	-	-	2.11	-	-	✓ Front	LIT	-	Hong Kong	China	[71]	-
34		11	6	6	-	2.11	-	-	✓ Hemispheric	EN-fm	4	Hong Kong	China	[37, 72]	-
35		15	-	-	-	2	-	-	-	EN-fm	4	Hong Kong	China	[65]	-
36		15.6	-	-	-	1.93	-	-	-	FM	-	Hong Kong	China	[65]	Raw data from measurement
37		13.0	4.0	4.4	23	1.52	-	-	✓ Hemispheric	FM	-	Hong Kong	China	[66]	-
38	*Casuarina equisetifolia*	8.0	7.2	-	-	1.52	-	-	✓ Front	LIT	-	Hong Kong	China	[71]	-
39		14.0 ± 5.9	-	-	45 ± 24	1.7 ± 0.5	-	-	-	FM	-	Greater Sydney	Australia	[73]	Sample size = 58
40		14	7	4	-	1.52	-	-	✓ Hemispheric	EN-fm	4	Hong Kong	China	[37, 72]	-
41		10	-	-	-	2.5	-	-	-	EN-fm	4	Hong Kong	China	[65]	-
42		10.8	-	-	-	2.46	-	-	-	FM	-	Hong Kong	China	[65]	Raw data from measurement
43		9.0	7.0	2.6	20	2.77	-	-	✓ Hemispheric	FM	-	Hong Kong	China	[66]	-
44	*Aleurites moluccana*	6.0	6.8	-	-	2.77	-	-	✓ Front	LIT	-	Hong Kong	China	[71]	-
45		10	7	3	-	3.10	-	-	✓ Hemispheric	EN-fm	4	Hong Kong	China	[37, 72]	-
46		9	7	3	-	2.77	-	-	✓ Hemispheric	EN-fm	4	Hong Kong	China	[37, 72]	-
47		9	7	3	-	2.77	-	-	-	EN-set	4.3	Hong Kong	China	[74]	-

48	*Ficus virens*	5 – 6	3 – 4	-	-	2.36 (summer) 1.32 (autumn) 0.78 (winter)	-	-	-	EN-fm	4.3.2	Shenzhen	China	[70]	-
49	*Lagerstroemia speciosa*	7.5	-	-	-	3	-	-	-	EN-fm	4	Hong Kong	China	[65]	-
50		6.5	-	-	-	2.98	-	-	-	FM	-	Hong Kong	China	[65]	Raw data from measurement
51	*Sterculia lanceolata*	8 – 10	-	-	-	1.16 – 1.72	-	-	-	EN-fm	4.4.4	Guangzhou	China	[69]	-
52	*Cinnamomum camphora*	10	-	-	-	3	-	-	-	EN-fm	4	Hong Kong	China	[65]	-
53		8.8	-	-	-	3.05	-	-	-	FM	-	Hong Kong	China	[65]	Raw data from measurement
54		10 – 20	-	-	-	1.77 – 3.03	-	-	-	EN-fm	≥4	Guangzhou	China	[68]	-
55		10 – 20	-	-	-	1.77 – 3.03	-	-	-	EN-fm	4.4.4	Guangzhou	China	[69]	-
56		13.3 ± 2.7	-	-	72 ± 20	1.9 ± 0.5	-	-	-	FM	-	Greater Sydney	Australia	[73]	Sample size =48 Named as Camphor laurel in the original literature
57		8	7	-	-	3.80	-	-	-	EN-fm	4	Wuhan	China	[75]	-
58		15	8	-	-	-	1.80	-	-	EN-fm	4	Changsha	China	[16]	-
59	*Delonix regia*	10	-	-	-	2.5	-	-	-	EN-fm	4	Hong Kong	China	[65]	-
60		9.7	-	-	-	2.52	-	-	-	FM	-	Hong Kong	China	[65]	Raw data from measurement
61		4.4	12.0	2.0	35	1.91	-	-	✓ Hemispheric	FM	-	Hong Kong	China	[66]	-
62		6.7	9.4	-	-	1.91	-	-	✓ Front	LIT	-	Hong Kong	China	[71]	-
63		8.86	6.21	-	28	2.5	-	-	✓ Front	LIT	-	Hong Kong	China	[67]	LAI in Open canopy
64		5 – 20	-	-	-	0.41 – 1.09	-	-	-	EN-fm	≥4	Guangzhou	China	[68]	-
65		5 – 20	-	-	-	0.41 – 1.09	-	-	-	EN-fm	4.4.4	Guangzhou	China	[69]	-
66	*Lophostemon confertus*	12.5 ± 6.9	-	-	35 ± 33	2.1 ± 0.4	-	-	✓ Front	FM	-	Greater Sydney	Australia	[73]	Sample size =49
67	*Melaleuca leucadendron*	10.6	6.0	3.2	43	3.42	-	-	✓ Hemispheric	FM	-	Hong Kong	China	[66]	-
68		11	6	3	-	3.42	-	-	✓ Hemispheric	EN-fm	4	Hong Kong	China	[37, 72]	-

Note: In the data source category, *FM* means direct measurements, *EN* means ENVI-met studies, and *LIT* means from previous literature or external databases. *Fm, lit, set, and mix,* respectively, means the data sources of the original ENVI-met study of field measurements, literature, and values set based on study foci and mixed sources. *No* means that data sources are not explicitly mentioned.

5.2. Green roof/façade model library

An ENVI-met green roof/façade model library for the common roof/façade greenings recommended by *the Hong Kong Greening and Landscape Office* is displayed in Table 6. The plant album is shown in Fig. 9, and the photo source is *Pictorial Guide to Plant Resources for Skyrise Greenery in Hong Kong*. Based on the sensitivity tests, LAI, leaf angle distribution, albedo, and transmittance values were microclimate-sensitive and should be included in the library. LAI values were ascertained due to its wide acquisition and use in greenery and microclimate studies. Very few studies reported leaf angle distribution, and only three records were found for *Funkia sp.* (Hosta) (0.5) [76] and *Hedera helix* (0.7) [77, 78]. Despite the fundamental importance of leaf angle distribution, Wang et al. [56] stated that its field measurements are laborious, requiring repeated determinations as the canopy develops. Muller-Linow et al. [79] found that no single method could meet all the requirements of leaf angle distribution measurement, such as easy applications under field conditions, the ability to measure changing canopies moved by wind, and the delivery of large sample size and high spatial resolution. Consequently, measuring a limited sample size by labor-intensive manual methods (such as using an inclinometer) under laboratory conditions may offer a possible solution. Otherwise, datasets or literature from other climate zones could be adopted as alternatives, but their appropriateness should be carefully reconsidered. For example, an Australian dataset includes measured leaf angle distribution of some climbers and ferns [56].

Regarding leaf albedo and transmittance, their values were relatively less well-documented. Only one study reported leaf transmittance (0.3, *Funkia sp.* (Hosta) [76] (listed in Appendix G). Some studies measured the collective reflectivity and transmissivity of plant leaves of the whole green façade rather than individual leaves. For example, a green façade reflectivity of 0.13, 0.22, and 0.26 were reported by [80-82]. However, due to the gaps among leaves, the albedo of a single leaf should be relatively larger than a group of plant leaves. Moreover, the leaf properties may vary at different phenological stages [83], so using such data in the literature demands careful consideration.

Since roof/façade greening properties are relatively less documented, only one-third of the plant species recommended by *the Hong Kong Greening and Landscape Office* are listed in the proposed library.

Therefore, users can consult information from other climate regions or consider other plant species in the subtropical humid climate region (*Cfa*). The alternative library is listed in Appendix G.

Fig. 9 Roof/façade greening album for the common species planted in subtropical South China.

Table 6. An ENVI-met roof/façade greening model library for the common plant species planted in subtropical South China.

No.	Plant growth form	Plant species	Plant height (m)	LAI (m^2/m^2)	Tree photo in the original literature	Measured city	Measured country	Ref.	Note
1	Climber	*Epipremnum aureum*	0.25-0.35	2.27	✓	Wuhan	China	[84]	-
2	Climber	*Lonicera japonica*	-	0.24	-	Hong Kong	China	[85]	-
3			-	0.69	-	Hong Kong	China	[86]	-
4			-	0.70	-	Hong Kong	China	[87]	LAI 0.695 in the original literature
5	Climber	*Pyrostegia venusta*	-	4.51 ± 0.033 (3-day mean)	✓	Guangzhou	China	[81]	-
6	Climber	*Wisteria sinensis*	-	0.95	-	Hong Kong	China	[88]	LAI 0.945 in the original literature
7	Succulent	*Sedum lineare*	0.07	4.6	-	Guangzhou	China	[89]	Rooftop greening
8			0.1 (summer) 0.02 (winter)	3.7 (summer) 0.2 (winter)	-	Shanghai	China	[90]	Rooftop greening
9			0.1 both	3.9 (no aquifer) 4.1 (with aquifer)	✓	Nanning	China	[91]	Rooftop greening
10			-	2.9	-	Chongqing	China	[92]	Rooftop greening
11			0.08 (mean)	2.6	-	Nanjing	China	[93]	Rooftop greening
12			0.08 (mean)	2.6	-	Nanjing	China	[94]	Rooftop greening
13			-	0.88	-	Shenzhen	China	[95]	Rooftop greening

14	Grass	*Cynodon dactylon*	-	4.45 ± 1.72 (the whole growing season)	-	-	China	[96]	Seasonal variations in LAI listed in the original literature
15			-	2.21±0.16	-	-	Japan	[97]	Rooftop greening
16	Grass	*Zoysia japonica*	-	1.55 ± 0.20	-	Kinkazan	Japan	[98]	*Zoysia japonica* was the only dominant, but several other species occurred, all with small to tiny plants
17	Fern	*Nephrolepis auriculata*	-	2.88 ± 0.63 (40% fern cover) 3.05 ± 0.50 (80% fern cover)	-	Hong Kong	China	[99]	-

Note: The default data source in this library is actual measurements. Data extracted from previous ENVI-met studies are noted.

6. Conclusion

This study aimed to formulate strategies for ENVI-met vegetation modeling to boost modeling data quality, simulation veracity, and rigor of ENVI-met studies. A series of sensitivity tests were conducted to investigate the microclimate-sensitive parameters and their influence on microclimate at the pedestrian level. For the microclimate-sensitive parameters in tree and roof/façade greening modeling, an ENVI-met vegetation model library focusing on species commonly planted in cities in subtropical South China was offered for users' reference. The main conclusions and modeling strategies are given below.

In ENVI-met tree modeling, LAD is the most significant parameter. It has a much greater impact on almost all microclimate variables at the pedestrian level (except air temperature) than foliage shortwave albedo and transmittance. Since LAD is commonly estimated by tree height and LAI, using accurate tree physical traits and LAI values would be strongly recommended to improve simulation accuracy. Some compromises on roof properties' input accuracy could be tolerant since they would not considerably hamper the overall simulation quality at the pedestrian level. When relevant literature and professional instruments are lacking, ENVI-met default values can be used as root properties.

Three strands of information demand attention in ENVI-met green roof/façade modeling. First, as a green roof/façade entity, only the simple plants' albedo, transmittance, and CO_2 fixation type significantly influence the simulation processes. The values of root zone depth, LAD profile, and RAD profile are neglected. Second, regarding roof/façade greening properties, LAI and leaf angle distribution are significant and should be accurately input to ensure simulation quality. Third, substrate properties affect the microclimate but are less influential than vegetation properties. Substrate emissivity greatly impacts building wall surface temperature, and an accurate value should be used in relevant studies. The sensitivity test results can be used as references in data analysis for the impact of modeling approximations. It should be noted that the results are based on hot and humid meteorological conditions, and their appropriateness should be carefully assessed before applying in other climate regions.

A seminal ENVI-met vegetation model library was developed, including a tree model part and a green roof/façade model part. In the library, data on fundamental plant physical traits, plant albums, and the essential parameter LAI were ascertained so that users could build a basic model. The vegetation model library can augment the microclimate research tools. It can be regarded as a helpful and actionable package through which researchers can quickly obtain accurate tree models without needing professional knowledge or instruments. It can also be beneficial for a more accurate understanding of the cooling role of greening in a local urban environment. Although this study only focused on commonly-used plant species in subtropical South China, it furnished an innovative and systematic workflow of vegetation model library development (Fig. 2) reproducible for implementation in other climate regions.

The current vegetation model library is in its preliminary stage of development and has some limitations. For instance, only the availability of data on LAI in the library can be ensured. However, in the case of foliage shortwave albedo or leaf angle distribution, which are also sensitive to microclimate, precise reference values for all plant species cannot be offered currently due to insufficient literature data. Addressing this limitation will be one of the future directions for developing the database.

Regarding reporting modeling information in manuscripts, this study suggested reporting values and corresponding data sources as detailed as possible. The essential information such as modeling settings, values, and data sources are valuable for future researchers, reuse, repurposing, and meta-analysis. Considering the word limit in journals, this study proposed at least reporting information on the essential plant physical traits and the microclimate-sensitive parameters comprehensively. Showing photographs of sample trees in a perspective view is recommended, supplementing details at the pedestrian level and providing a visual reference to readers. Evaluating the tree images can also help researchers judge whether the models in previous studies are applicable and suitable to their work.

For future studies, collaborating with experts and professional research teams in botany and dendrology can provide an optimal direction and more accurate measured values for library improvement. Tree albums that focus on trees' 3D shape (for example, a library of *Lindenmayer-System* trees) can be another feasible direction for library improvement. Substrate properties also deserve more future studies. Due to the considerable diversity of green roof/façade substrate materials and time limitations, the proposed model library mainly focused on plant-related parameters with little information on substrate properties. The substrate's microclimatic effects have been verified in the sensitivity tests. Therefore, its properties can provide a valuable direction for future library development studies.

Acknowledgments

This research is supported by the General Research Fund (RGC Ref No. 14617220) from the Research Grants Council (RGC) of Hong Kong.

References

1. Santamouris, M., *Regulating the damaged thermostat of the cities—Status, impacts and mitigation challenges.* Energy and Buildings, 2015. **91**: 43-56.
2. He, B.-J., J. Wang, H. Liu, and G. Ulpiani, *Localized synergies between heat waves and urban heat islands: Implications on human thermal comfort and urban heat management.* Environmental Research, 2021. **193**: 110584.
3. Salmond, J.A., M. Tadaki, S. Vardoulakis, K. Arbuthnott, A. Coutts, M. Demuzere, K.N. Dirks, C. Heaviside, S. Lim, and H. Macintyre, *Health and climate related ecosystem services provided by street trees in the urban environment.* Environmental Health, 2016. **15**(1): 95-111.
4. Wong, N.H., C.L. Tan, D.D. Kolokotsa, and H. Takebayashi, *Greenery as a mitigation and adaptation strategy to urban heat.* Nature Reviews Earth & Environment, 2021. **2**(3): 166-181.

5. Liu, Z., W. Cheng, C.Y. Jim, T.E. Morakinyo, Y. Shi, and E. Ng, *Heat mitigation benefits of urban green and blue infrastructures: A systematic review of modeling techniques, validation and scenario simulation in ENVI-met V4.* Building and Environment, 2021. **200**: 107939.
6. Yang, Y., E. Gatto, Z. Gao, R. Buccolieri, T.E. Morakinyo, and H. Lan, *The "plant evaluation model" for the assessment of the impact of vegetation on outdoor microclimate in the urban environment.* Building and Environment, 2019. **159**: 106151.
7. Toparlar, Y., B. Blocken, B. Maiheu, and G.J.F. van Heijst, *A review on the CFD analysis of urban microclimate.* Renewable and Sustainable Energy Reviews, 2017. **80**: 1613-1640.
8. Bruse, M. and H. Fleer, *Simulating surface–plant–air interactions inside urban environments with a three dimensional numerical model.* Environmental Modelling & Software, 1998. **13**(3-4): 373-384.
9. Bruse, M., *ENVI-met implementation of the Jacobs A− gs Model to calculate the stomata conductance*. 2004, Bochum.
10. Huttner, S., *Further development and application of the 3D microclimate simulation ENVI-met*. 2012, Johannes Gutenberg University of Mainz.
11. Helge, S., *Modeling urban microclimate: development, implementation and evaluation of new and improved calculation methods for the urban microclimate model ENVI-met*. 2016, Johannes Gutenberg University of Mainz.
12. Simon, H., T. Sinsel, and M. Bruse, *Introduction of Fractal-Based Tree Digitalization and Accurate In-Canopy Radiation Transfer Modelling to the Microclimate Model ENVI-met.* Forests, 2020. **11**(8): 869.
13. Liu, Z., S. Zheng, and L. Zhao, *Evaluation of the ENVI-Met vegetation model of four common tree species in a subtropical hot-humid area.* Atmosphere, 2018. **9**(5): 198.
14. Ouyang, W., T. Sinsel, H. Simon, T.E. Morakinyo, H. Liu, and E. Ng, *Evaluating the thermal-radiative performance of ENVI-met model for green infrastructure typologies: Experience from a subtropical climate.* Building and Environment, 2022. **207**: 108427.
15. Peel, M.C., B.L. Finlayson, and T.A. McMahon, *Updated world map of the Köppen-Geiger climate classification.* Hydrology and Earth System Sciences, 2007. **11**(5): 1633-1644.
16. Chen, Y., B. Zheng, and Y. Hu, *Numerical simulation of local climate zone cooling achieved through modification of trees, albedo and green roofs-a case study of changsha, China.* Sustainability (Basel, Switzerland), 2020. **12**(7): 2752.
17. Eksi, M., D.B. Rowe, I.S. Wichman, and J.A. Andresen, *Effect of substrate depth, vegetation type, and season on green roof thermal properties.* Energy and Buildings, 2017. **145**: 174-187.
18. Ng, E., L. Chen, Y. Wang, and C. Yuan, *A study on the cooling effects of greening in a high-density city: An experience from Hong Kong.* Building and environment, 2012. **47**: 256-271.
19. Lee, Y., J.J. Filliben, R.J. Micheals, and P.J. Phillips, *Sensitivity analysis for biometric systems: A methodology based on orthogonal experiment designs.* Computer Vision and Image Understanding, 2013. **117**(5): 532-550.
20. Yuan, C. and E. Ng, *Practical application of CFD on environmentally sensitive architectural design at high density cities: A case study in Hong Kong.* Urban Climate, 2014. **8**: 57-77.
21. Czitrom, V., *One-factor-at-a-time versus designed experiments.* The American Statistician, 1999. **53**(2): 126-131.
22. Chau, N., C.Y. Jim, and H. Zhang, *Species-specific holistic assessment of tree structure and defects in urban Hong Kong.* Urban Forestry & Urban Greening, 2020. **55**: 126813.
23. Zhang, H. and C.Y. Jim, *Contributions of landscape trees in public housing estates to urban biodiversity in Hong Kong.* Urban Forestry & Urban Greening, 2014. **13**(2): 272-284.
24. *Street Tree Selection Guide*. 2018, Development Bureau. The Greening, Landscape, and Tree Management Section. The government of the Hong Kong Special Administrative Region.
25. Jones, H.G., *Plants and microclimate: a quantitative approach to environmental plant physiology*. 2013: Cambridge University Press.

26. Liu, Z., R.D. Brown, S. Zheng, Y. Jiang, and L. Zhao, *An in-depth analysis of the effect of trees on human energy fluxes.* Urban Forestry & Urban Greening, 2020. **50**: 126646.
27. Morakinyo, T.E., L. Kong, K.K.-L. Lau, C. Yuan, and E. Ng, *A study on the impact of shadow-cast and tree species on in-canyon and neighborhood's thermal comfort.* Building and Environment, 2017. **115**: 1.
28. Morakinyo, T.E., K.K.-L. Lau, C. Ren, and E. Ng, *Performance of Hong Kong's common trees species for outdoor temperature regulation, thermal comfort and energy saving.* Building and Environment, 2018. **137**: 157.
29. He, Y., E.S. Lin, W. Zhang, C.L. Tan, P.Y. Tan, and N.H. Wong, *Local microclimate above shrub and grass in tropical city: A case study in Singapore.* Urban Climate, 2022. **43**: 101142.
30. Sinsel, T., H. Simon, A.M. Broadbent, M. Bruse, and J. Heusinger, *Modeling the outdoor cooling impact of highly radiative "super cool" materials applied on roofs.* Urban Climate, 2021. **38**: 100898.
31. Höppe, P., *The physiological equivalent temperature–a universal index for the biometeorological assessment of the thermal environment.* International Journal of Biometeorology, 1999. **43**(2): 71-75.
32. Mayer, H. and P. Höppe, *Thermal comfort of man in different urban environments.* Theoretical and applied climatology, 1987. **38**(1): 43-49.
33. Bochenek, A.D. and K. Klemm, *The Impact of Passive Green Technologies on the Microclimate of Historic Urban Structures: The Case Study of Lodz.* Atmosphere, 2020. **11**(9): 974.
34. Lee, H., H. Mayer, and W. Kuttler, *Impact of the spacing between tree crowns on the mitigation of daytime heat stress for pedestrians inside E-W urban street canyons under Central European conditions.* Urban forestry & urban greening, 2020. **48**.
35. Sodoudi, S., H. Zhang, X. Chi, F. Müller, and H. Li, *The influence of spatial configuration of green areas on microclimate and thermal comfort.* Urban forestry & urban greening, 2018. **34**: 85-96.
36. Knaus, M. and D. Haase, *Green roof effects on daytime heat in a prefabricated residential neighbourhood in Berlin, Germany.* Urban Forestry and Urban Greening, 2020. **53**.
37. Morakinyo, T.E., K.K.-L. Lau, C. Ren, and E. Ng, *Performance of Hong Kong's common trees species for outdoor temperature regulation, thermal comfort and energy saving.* Building and environment, 2018. **137**: 157-170.
38. Morakinyo, T.E., A. Lai, K.K.-L. Lau, and E. Ng, *Thermal benefits of vertical greening in a high-density city: Case study of Hong Kong.* Urban Forestry & Urban Greening, 2019. **37**: 42-55.
39. Lan, H., K.K.-L. Lau, Y. Shi, and C. Ren, *Improved urban heat island mitigation using bioclimatic redevelopment along an urban waterfront at Victoria Dockside, Hong Kong.* Sustainable Cities and Society, 2021. **74**: 103172.
40. Tan, Z., K.K.-L. Lau, and E. Ng, *Urban tree design approaches for mitigating daytime urban heat island effects in a high-density urban environment.* Energy and Buildings, 2016. **114**: 265-274.
41. Morakinyo, T.E., W. Ouyang, K.K.-L. Lau, C. Ren, and E. Ng, *Right tree, right place (urban canyon): Tree species selection approach for optimum urban heat mitigation - development and evaluation.* Science of The Total Environment, 2020. **719**: 137461.
42. Tan, Z., K.K.-L. Lau, and E. Ng, *Planning strategies for roadside tree planting and outdoor comfort enhancement in subtropical high-density urban areas.* BUILD ENVIRON, 2017. **120**: 93-109.
43. Jim, C.Y., *Roadside trees in urban Hong Kong: Part II Species Composition.* Arboricultural Journal, 1996. **20**(3): 279-298.
44. Jim, C.Y., *Trees in major urban parks in Hong Kong*, ed. C. Green Hong Kong, L. Hong Kong, and D. Cultural Services. 2000, Hong Kong: Green Hong Kong Campaign : Leisure and Cultural Services Dept.
45. Jim, C.Y., *Street trees in high-density urban Hong Kong.* Journal of Arboriculture, 1986. **12**(10): 257-263.

46. Jim, C.Y., *Roadside trees in urban Hong Kong: Part I census methodology.* Arboricultural Journal, 1996. **20**(2): 221-237.
47. Jim, C.Y., *Multipurpose census methodology to assess urban forest structure in Hong Kong.* Arboriculture and Urban Forestry, 2008. **34**(6): 366-378.
48. Jim, C.Y. and H. Zhang, *Species diversity and spatial differentiation of old-valuable trees in urban Hong Kong.* Urban Forestry & Urban Greening, 2013. **12**(2): 171-182.
49. Lee, L.S., C.Y. Jim, and H. Zhang, *Tree density and diversity in Hong Kong's public housing estates: From provision injustice to socio-ecological inclusiveness.* Urban Forestry & Urban Greening, 2019. **46**: 126468.
50. Jim, C.Y. and H. Liu, *Species diversity of three major urban forest types in Guangzhou City, China.* Forest Ecology and Management, 2001. **146**(1-3): 99-114.
51. *Pictorial Guide to Plant Resources for Skyrise Greenery in Hong Kong*. 2013, Greening, Landscape and Tree Management Section Development Bureau, The Government of the Hong Kong Special Administrative Region. https://www.greening.gov.hk/en/greening-landscape/right-plant-right-place/skyrise-greenery/pictorial-guide-to-plant-resources-for-skyrise-gre/index.html.
52. Pedruzo-Bagazgoitia, X., H. Ouwersloot, M. Sikma, C. Van Heerwaarden, C. Jacobs, and J. Vilà-Guerau de Arellano, *Direct and diffuse radiation in the shallow cumulus–vegetation system: Enhanced and decreased evapotranspiration regimes.* Journal of Hydrometeorology, 2017. **18**(6): 1731-1748.
53. Brown, R.D. and T.J. Gillespie, *Microclimatic landscape design: creating thermal comfort and energy efficiency*. Vol. 1. 1995: Wiley New York.
54. Sinsel, T., H. Simon, W. Ouyang, C. dos Santos Gusson, P. Shinzato, and M. Bruse, *Implementation and evaluation of mean radiant temperature schemes in the microclimate model ENVI-met.* Urban Climate, 2022. **45**: 101279.
55. Liu, Z., R.D. Brown, S. Zheng, L. Zhang, and L. Zhao, *The effect of trees on human energy fluxes in a humid subtropical climate region.* International Journal of Biometeorology, 2020. **64**(10): 1675-1686.
56. Wang, W.-M., Z.-L. Li, and H.-B. Su, *Comparison of leaf angle distribution functions: Effects on extinction coefficient and fraction of sunlit foliage.* Agricultural and Forest Meteorology, 2007. **143**(1-2): 106-122.
57. Hui, L., C.Y. Jim, and H. Zhang, *Allometry of urban trees in subtropical Hong Kong and effects of habitat types.* Landscape Ecology, 2020. **35**(5): 1143-1160.
58. Lalic, B. and D.T. Mihailovic, *An empirical relation describing leaf-area density inside the forest for environmental modeling.* Journal of Applied Meteorology, 2004. **43**(4): 641-645.
59. Fahmy, M., H. El-Hady, M. Mahdy, and M.F. Abdelalim, *On the green adaptation of urban developments in Egypt; predicting community future energy efficiency using coupled outdoor-indoor simulations.* Energy and Buildings, 2017. **153**: 241-261.
60. Fahmy, M., Y. Ibrahim, E. Hanafi, and M. Barakat, *Would LEED-UHI greenery and high albedo strategies mitigate climate change at neighborhood scale in Cairo, Egypt?* Building Simulation, 2018. **11**(6): 1273-1288.
61. Fabbri, K., G. Canuti, and A. Ugolini, *A methodology to evaluate outdoor microclimate of the archaeological site and vegetation role: A case study of the Roman Villa in Russi (Italy).* Sustainable Cities and Society, 2017. **35**: 107-133.
62. Jacquemoud, S. and L. Ustin, *Modeling leaf optical properties.* Photobiological Sciences Online, 2008.
63. Pavan, G., S. Jacquemoud, G. De Rosny, J. Rambaut, J. Frangi, L. Bidel, and C. François. *Ramis: A new portable field radiometer to estimate leaf biochemical content*. In *Seventh international conference on precision agriculture and other precision resources management*. 2004. Citeseer.
64. Bruse, M., *ENVI-met implementation of the gas/particle dispersion and deposition model PDDM.* Envi-met. com, 2007.

65. Xing, Y., P. Brimblecombe, S. Wang, and H. Zhang, *Tree distribution, morphology and modelled air pollution in urban parks of Hong Kong.* Journal of Environmental Management, 2019. **248**: 109304.
66. Kong, L., K.K.-L. Lau, C. Yuan, Y. Chen, Y. Xu, C. Ren, and E. Ng, *Regulation of outdoor thermal comfort by trees in Hong Kong.* Sustainable Cities and Society, 2017. **31**: 12-25.
67. Wang, Z., Y. Li, J. Song, K. Wang, J. Xie, P.W. Chan, C. Ren, and S. Di Sabatino, *Modelling and optimizing tree planning for urban climate in a subtropical high-density city.* Urban Climate, 2022. **43**: 101141.
68. Li, J., Y. Wang, Z. Ni, S. Chen, and B. Xia, *An integrated strategy to improve the microclimate regulation of green-blue-grey infrastructures in specific urban forms.* Journal of cleaner production, 2020. **271**: 122555.
69. Wang, Y., Z. Ni, M. Hu, S. Chen, and B. Xia, *A practical approach of urban green infrastructure planning to mitigate urban overheating: A case study of Guangzhou.* Journal of cleaner production, 2021. **287**: 124995.
70. Wang, Y., Z. Ni, S. Chen, and B. Xia, *Microclimate regulation and energy saving potential from different urban green infrastructures in a subtropical city.* Journal of cleaner production, 2019. **226**: 913-927.
71. Huang, X., J. Song, C. Wang, T.F.M. Chui, and P.W. Chan, *The synergistic effect of urban heat and moisture islands in a compact high-rise city.* Building and Environment, 2021. **205**: 108274.
72. Morakinyo, T.E., L. Kong, K.K.-L. Lau, C. Yuan, and E. Ng, *A study on the impact of shadow-cast and tree species on in-canyon and neighborhood's thermal comfort.* Building and environment, 2017. **115**: 1-17.
73. T.U.N., K., T. M.G., and P. S., *Temperature Reduction in Urban Surface Materials through Tree Shading Depends on Surface Type Not Tree Species.* Forests, 2020. **11**(11): 1141.
74. Ouyang, W., T.E. Morakinyo, C. Ren, and E. Ng, *The cooling efficiency of variable greenery coverage ratios in different urban densities: A study in a subtropical climate.* Building and Environment, 2020. **174**: 106772.
75. Zhang, L., Q. Zhan, and Y. Lan, *Effects of the tree distribution and species on outdoor environment conditions in a hot summer and cold winter zone: A case study in Wuhan residential quarters.* Building and environment, 2018. **130**: 27-39.
76. Zheng, B., J. Li, X. Chen, and X. Luo, *Evaluating the Effects of Roof Greening on the Indoor Thermal Environment throughout the Year in a Chinese City (Chenzhou).* Forests, 2022. **13**(2): 304.
77. Li, J., B. Zheng, W. Shen, Y. Xiang, X. Chen, and Z. Qi, *Cooling and energy-saving performance of different green wall design: A simulation study of a block.* Energies (Basel), 2019. **12**(15): 2912.
78. Li, J., B. Zheng, X. Chen, Z. Qi, K.B. Bedra, J. Zheng, Z. Li, and L. Liu, *Study on a full-year improvement of indoor thermal comfort by different vertical greening patterns.* Journal of Building Engineering, 2021. **35**: 101969.
79. Müller-Linow, M., F. Pinto-Espinosa, H. Scharr, and U. Rascher, *The leaf angle distribution of natural plant populations: assessing the canopy with a novel software tool.* Plant methods, 2015. **11**(1): 1-16.
80. Lee, L.S. and C.Y. Jim, *Transforming thermal-radiative study of a climber green wall to innovative engineering design to enhance building-energy efficiency.* Journal of Cleaner Production, 2019. **224**: 892-904.
81. Zhang, L., Z. Deng, L. Liang, Y. Zhang, Q. Meng, J. Wang, and M. Santamouris, *Thermal behavior of a vertical green facade and its impact on the indoor and outdoor thermal environment.* Energy and buildings, 2019. **204**: 109502.
82. Zazzini, P. and G. Grifa, *Energy Performance Improvements in Historic Buildings by Application of Green Walls: Numerical Analysis of an Italian Case Study.* Energy Procedia, 2018. **148**: 1143-1150.

83. Oguntunde, P.G. and N. Van De Giesen, *Crop growth and development effects on surface albedo for maize and cowpea fields in Ghana, West Africa.* International Journal of Biometeorology, 2004. **49**(2): 106-112.
84. Cao, Y., F. Li, Y. Wang, Y. Yu, Z. Wang, X. Liu, and K. Ding, *Assisted deposition of PM2. 5 from indoor air by ornamental potted plants.* Sustainability, 2019. **11**(9): 2546.
85. Lee, L.S.H. and C.Y. Jim, *Energy benefits of green-wall shading based on novel-accurate apportionment of short-wave radiation components.* Applied energy, 2019. **238**: 1506-1518.
86. Lee, L.S.H. and C.Y. Jim, *Transforming thermal-radiative study of a climber green wall to innovative engineering design to enhance building-energy efficiency.* Journal of cleaner production, 2019. **224**: 892-904.
87. Lee, L.S.H. and C.Y. Jim, *Multidimensional analysis of temporal and layered microclimatic behavior of subtropical climber green walls in summer.* Urban ecosystems, 2019. **23**(2): 389-402.
88. Lee, L.S. and C.Y. Jim, *Multidimensional analysis of temporal and layered microclimatic behavior of subtropical climber green walls in summer.* Urban Ecosystems, 2020. **23**(2): 389-402.
89. Feng, C., Q. Meng, and Y. Zhang, *Theoretical and experimental analysis of the energy balance of extensive green roofs.* Energy and buildings, 2010. **42**(6): 959-965.
90. He, Y., H. Yu, A. Ozaki, and N. Dong, *Thermal and energy performance of green roof and cool roof: A comparison study in Shanghai area.* Journal of Cleaner Production, 2020. **267**: 122205.
91. Zhang, K., A. Garg, G. Mei, M. Jiang, H. Wang, S. Huang, and L. Gan, *Thermal performance and energy consumption analysis of eight types of extensive green roofs in subtropical monsoon climate.* Building and Environment, 2022. **216**: 108982.
92. Gao, Y., D. Shi, R. Levinson, R. Guo, C. Lin, and J. Ge, *Thermal performance and energy savings of white and sedum-tray garden roof: A case study in a Chongqing office building.* Energy and Buildings, 2017. **156**: 343-359.
93. Yin, H., F. Kong, I. Dronova, A. Middel, and P. James, *Investigation of extensive green roof outdoor spatio-temporal thermal performance during summer in a subtropical monsoon climate.* The Science of the total environment, 2019. **696**: 133976-133976.
94. Liu, H., H. Yin, F. Kong, A. Middel, X. Zheng, J. Huang, T. Sun, D. Wang, and I.M. Lensky, *Change of nutrients, microorganisms, and physical properties of exposed extensive green roof substrate.* The Science of the total environment, 2022. **805**: 150344-150344.
95. Li, S., H. Qin, Y.N. Peng, and S.T. Khu, *Modelling the combined effects of runoff reduction and increase in evapotranspiration for green roofs with a storage layer.* Ecological Engineering, 2019. **127**: 302-311.
96. Wen, Z., M. Ma, C. Zhang, X. Yi, J. Chen, and S. Wu, *Estimating seasonal aboveground biomass of a riparian pioneer plant community: An exploratory analysis by canopy structural data.* Ecological Indicators, 2017. **83**: 441-450.
97. Kuronuma, T., H. Watanabe, T. Ishihara, D. Kou, K. Toushima, M. Ando, and S. Shindo, *CO2 Payoff of Extensive Green Roofs with Different Vegetation Species.* Sustainability (Basel, Switzerland), 2018. **10**(7): 2256.
98. Werger, M.J.A., T. Hirose, H.J. During, G.W. Heil, K. Hikosaka, T. Ito, U.G. Nachinshonhor, D. Nagamatsu, K. Shibasaki, S. Takatsuki, J.W. van Rheenen, and N.P.R. Anten, *Light partitioning among species and species replacement in early successional grasslands.* Journal of vegetation science, 2002. **13**(5): 615-626.
99. Chau, N.L. and L. Chu, *Fern cover and the importance of plant traits in reducing erosion on steep soil slopes.* Catena (Giessen), 2017. **151**: 98-106.

Highlights

- The input accuracy of LAD is most influential to the overall simulation accuracy
- High tolerance is acceptable for errors of input parameter trees' roof properties
- LAI and leaf angle distribution of green roof & façade are important for simulation
- Substrate properties of green roof & façade have limited influence on microclimate
- Proposed a systematic workflow to develop an ENVI-met vegetation model library

Declaration of interests

☒ The authors declare that they have no known competing financial interests or personal relationships that could have appeared to influence the work reported in this paper.

☐The authors declare the following financial interests/personal relationships which may be considered as potential competing interests: